IJCA

Indonesian Journal of Chemical Analysis

Homepage: https://journal.uii.ac.id/IJCA

Evaluation of the Chemical Structure and Thermal Properties of Polyethylene Glycol (PEG)-Doped Polylactic Acid (PLA)/Multiwalled Carbon Nanotube (MWCNT) Composites

Awaludin Fitroh Rifa'i*, Mujtahid Kaavessina, Sperisa Distantina

Department of Chemical Engineering, Faculty of Engineering, Universitas Sebelas Maret, Surakarta, 57126, Indonesia
* corresponding author: awaludin21fitroh@gmail.com
DOI: 10.20885/ijca.vol7.iss2.art5

GRAPHICAL ABSTRACT

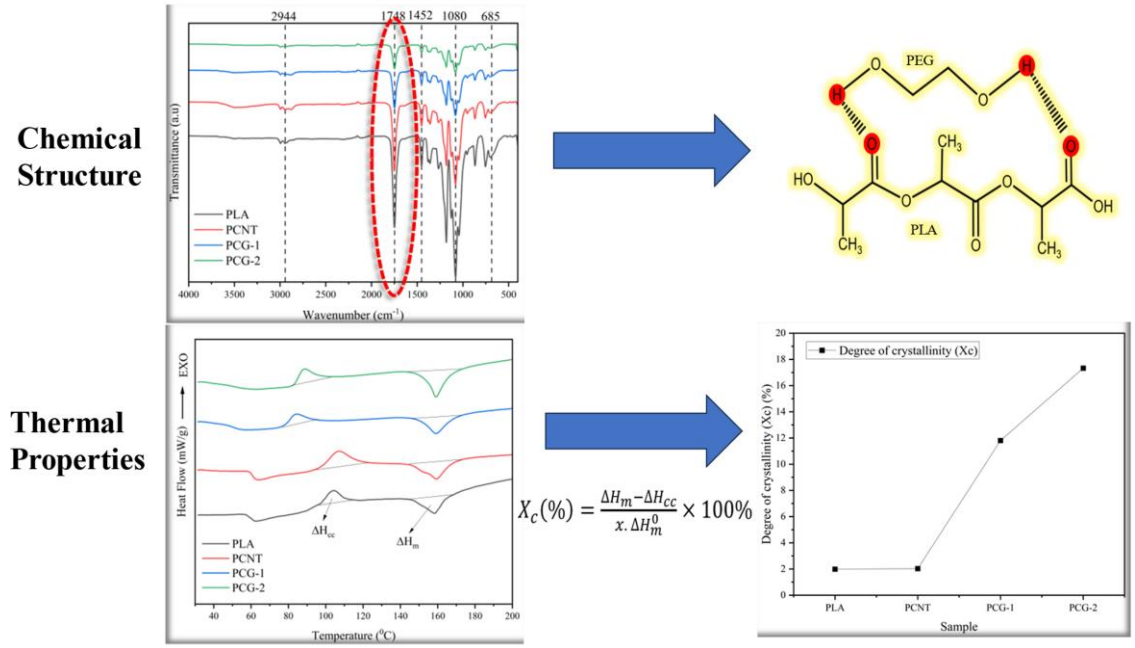

ARTICLE INFO

Received : 22 June 2024
Revised : 12 August 2024
Published : 30 September 2024
Keywords : polylactic acid, polyethylene glycol, masterbatch blending, ATR-FTIR, TGA-DSC

ABSTRACT

This study aimed to investigate the chemical structure, thermal properties, and stability of polylactic acid (PLA) composites blended with multi-walled carbon nanotubes (MWCNTs) and polyethylene glycol (PEG). The composites were fabricated using a masterbatch blending method with two different molecular weights (Mw) of PEG. The masterbatch was initially prepared using solvent casting with chloroform as the solvent, followed by melt blending using an extruder. ATR-FTIR spectroscopy identified strong hydrogen bonds between the C=O groups of PLA and the –OH groups of PEG, as evidenced by the peak at 1748 cm^{-1}. Differential Scanning Calorimetry (DSC) revealed that incorporating 14 wt% of PEG 10,000 into PLA/MWCNT composite significantly enhances the melting enthalpy (ΔH_m) from 18.3 J/g to 24.6 J/g and the degree of crystallinity from 2% to 17.3%. The glass transition temperature (T_g) decreased with the addition of PEG, indicating increased chain mobility, while the melting temperature (T_m) remained relatively constant around 158

°C regardless of the PEG Mw. Despite the plasticizing effect of PEG, the thermal stability of the composites was maintained across different PEG Mw. Scanning Electron Microscope (SEM) images showed that MWCNTs were well dispersed within the blend, facilitated by ultrasonic stirring during preparation.

1. INTRODUCTION

Biocompatible and biodegradable polymers have been extensively researched to address the increasing demand for the conservation of raw fossil materials and the promotion of sustainable green technologies [1, 2]. Despite their environmental benefits, the widespread adoption of these polymers is hindered by their high cost, limited thermostability, and suboptimal mechanical properties compared to those of conventional plastics derived from crude oil [3]. To mitigate these issues, blending polymers has emerged as a promising technique. By combining biopolymers with various synthetic and other biopolymers, researchers can develop new materials with tailored properties, potentially overcoming the performance limitations of individual biopolymers [4, 5].

Polylactic acid (PLA), derived from renewable natural sources, is a promising alternative to petroleum-based polymers due to its biocompatibility and biodegradability. However, the inherent brittleness of PLA has limited its widespread adoption in large-scale commercial applications. This brittleness leads to low toughness, impact strength, elongation at break, and subpar thermal properties, making it unsuitable for applications such as transportation that demand high-performance materials [6]. Therefore, integrating a suitable and compatible toughening agent is crucial for enhancing the mechanical properties of PLA. One effective approach to mitigate the brittleness of PLA is to blend it with polyethylene glycol (PEG).

PEG is a ductile and compatible polymer that enhances the flexibility and toughness of PLA. This makes PEG an effective plasticizing agent, addressing the mechanical limitations of PLA [7]. Chalid et al. [8] reported that adding PEG increased the crystallinity of the PLA; however, it resulted in a decrease in its hardness. Additionally, carbon nanotubes (CNTs) enhance composite materials because of their exceptional technical capabilities and fiber-like shapes. When used with biodegradable polymers for second-phase reinforcement, CNTs demonstrate excellent electrical, mechanical, thermal, and structural capabilities, sparking interest in both academic and industrial contexts [9]. Ahmad et al. [9] successfully synthesized MWCNT/PLA/PEG nanocomposites designed for electromagnetic interference (EMI) shielding applications using a combination of melt blending and hot-pressing techniques. Field emission scanning electron microscopy (FE-SEM) images demonstrated that the MWCNTs are typically curved and tangled with one another. Due to strong van der Waals interactions, MWCNT nanoparticles have a high tendency to form bundles. Furthermore, thermal stability tests revealed that the incorporation of MWCNTs slightly decreased the thermal stability of the MWCNT/PLA/PEG nanocomposites compared to that of the PLA/PEG composite. Wang et al. [10] developed MWCNT/PLA/PEG composites and found that the blended PEG might reduce the energy barrier, facilitating crystal formation and leading to a decrease in the cold crystallization temperature (T_{cc}) with increasing PEG content. Regarding differential scanning calorimetry (DSC) results, MWCNTs slightly increase the melting temperature (T_m) due to their entanglement effect, which requires higher energy to relax polymer chains. Furthermore, the addition of PEG influenced the glass transition temperature (T_g), while MWCNTs impacted T_{cc}, with minimal influence on T_m and degree of crystallinity (X_c) of the composites [11].

The melt blending method is widely used in polymer processing because it is efficient, economical, and easy to apply [12]. However, a significant challenge with this method is achieving the appropriate distribution and dispersion of CNTs within the polymer matrix. This difficulty makes directly mixing CNTs with the PLA matrix during melt blending problematic. Additionally, CNTs have low solubility in most organic solvents and PLA [13]. The melt blending method can be modified by creating a masterbatch to overcome these challenges. The masterbatch method provides the advantage of better dispersing CNTs within the polymer matrix. In previous research, functionalized graphene nanosheets (f-GNSs) were incorporated into PLA using the masterbatch premixing technique. This process involved using tetrahydrofuran (THF) as the solvent combined with sonication. After the solvent evaporated, the master batch and PLA were processed with a twin

roller mill at 80 rpm and then subjected to a hot press [14]. In addition to THF, PLA is also soluble in solvents such as dichloromethane or chloroform [7].

A comprehensive understanding of thermal analysis is essential for identifying the processing and recycling conditions of polymers and their mixtures. Thermogravimetric analysis (TGA) is an analytical technique used to measure the mass change of a sample as it undergoes a controlled temperature program. This method provides critical insights into the thermal stability of materials. When TGA is combined with differential scanning calorimetry (DSC), it allows for a comprehensive analysis by measuring both the heat flow and the mass change associated with thermal processes. By analyzing the heat flow associated with melting and crystallization, DSC provides detailed information on the thermal transitions and crystallization behavior of polymers [15]. Fourier transform infrared (FTIR) spectroscopy is a powerful technique used to determine the orientation and structure of crystalline polymer regions [16]. This approach allows for a detailed characterization of the polymer microstructure at the molecular level. FTIR is commonly employed to monitor conformational changes in polymer chains and to analyze the crystallization kinetics of semicrystalline polymers during their crystallization process [17, 18]. Additionally, FTIR can distinguish between different crystalline forms [19] and is utilized to observe changes in the orientation of both crystalline and amorphous phases during polymer deformation [20].

The current study aimed to analyze the spectroscopic structure, thermal properties, and stability of PLA/MWCNT/PEG composites. This analysis was conducted using the masterbatch blending method to understand the effects of PEG with different molecular weights (Mw: 1000 and 10,000 g/mol) on these composites, both before and after their addition. Masterbatches were prepared via solvent casting processes with chloroform as the solvent, and melt blending processes were continued using an extruder. The resulting polymer composites were characterized by ATR-FTIR, SEM, and TGA-DSC, including the determination of the degree of crystallinity.

2. EXPERIMENTAL METHODS

2.1. Materials

The materials used in this study were as follows: PLA granules, with a density of 1.24 g/cm³, were obtained from Xiamen Keyuan Plastic Co., Ltd. MWCNTs were obtained from Jiangsu XFNANO Materials Tech Co., Ltd., and had an electrical conductivity of approximately 100 S/cm, an outer diameter of 20-30 nm, a length of 0.5-2 μm, and a purity of more than 95%. The MWCNTs possess 23-25 walls and an aspect ratio of less than 100. PEGs with molecular weights of 1,000 and 10,000 g/mol were obtained from Sigma–Aldrich. Analytical grade chloroform, used as a solvent for casting polymer masterbatches, was supplied by Aldrich Co., Ltd. All materials were used as received without any additional purification processes.

2.2. Masterbatch Synthesis

Before processing, the PLA was dried overnight in an oven at 80 °C to remove moisture. To begin the solution preparation, 20% of the dried PLA was dissolved in 100 ml chloroform. This mixture was agitated using a magnetic stirrer set to 200 rpm at 55 °C until the PLA was completely dissolved. Next, PEG was added to the PLA solution at 0% and 14% weights. Simultaneously, an MWCNT suspension was prepared by dissolving 1% MWCNTs in 50 ml of chloroform. This suspension was then sonicated using a Kingqi Science sonicator (model: KQJS-800) at 50% power (P: 800 W) for 30 minutes to ensure uniform dispersion of the MWCNTs. The prepared MWCNT suspension was mixed with the PLA/PEG solution and stirred at 200 rpm for 30 minutes to create the master batch solution. This solution was then poured into molds and allowed to dry at room temperature for 12 hours.

2.3. Composite Preparation

The prepared masterbatches were dispersed into the PLA matrix with various PLA weight percentages of 79% and 65% using a Single Screw Extruder SJ25. The extrusion process involved maintaining specific temperature gradients across the zones: 100 °C in the initial heating zone, 170 °C in the second zone, and 165 °C in the third zone. The screw rotation speed was consistently set at 20 rpm. The filament was air-cooled during extrusion, resulting in a final average diameter of

approximately 1 mm. In parallel, pure PLA underwent the same melt treatment process to facilitate a comparison of its behavior before and after blending with MWCNTs and PEG. The PLA/MWCNT blend is called PCNT, while the PLA/MWCNT/PEG blends are denoted as PCG-1 for PEG 1,000 and PCG-2 for PEG 10,000.

2.4. Attenuated Total Reflectance Fourier Transform Infrared (ATR-FTIR) Spectroscopy

FTIR analysis was used to determine the functional groups of the PLA and PEGs, as well as the interactions and dispersion of PEG in the PLA polymer composites. A Perkin Elmer UATR Spectrum Two Spectrometer was used to measure the ATR-IR spectra at room temperature with a wavelength range of 400-4000 cm^{-1} and a scanning resolution of 4 cm^{-1}, which was carried out in transmittance mode.

2.5. Thermal Properties

The thermal properties of the samples were analyzed using a simultaneous differential thermal analysis–differential scanning calorimetry (TGA–DTG–DSC) thermogravimetric analyzer. These measurements were performed on a NEXTA STA (Hitachi STA200RV) instrument. Approximately 10 mg of each sample was used for the analysis. Thermal scanning was performed from 30 °C to 550 °C with a heating rate (β) of 10 °C/min. The experiments were conducted under a nitrogen atmosphere with a 100 mL/min flow rate to prevent oxidation and ensure an inert environment during the thermal analysis.

The thermal properties of the polymer composites were characterized with a thoroughness that left no room for doubt, using differential scanning calorimetry (DSC) analysis. This method was employed to further determine the degree of crystallinity (X_c). The value of X_c was determined using equation (1) [21]:

$$X_c(\%) = \frac{\Delta H_m - \Delta H_{cc}}{x.\ \Delta H_m^0} \times 100\% \quad (1)$$

where ΔH_m and ΔH_{cc} are the experimental melting and cold crystallization enthalpies, respectively. *x* is the weight fraction of the PLA in the composites. A value of $\Delta H_m^0 = 93.7$ J/g [6, 22] was used in the calculations, based on the melting enthalpy associated with 100% crystalline PLA.

The thermal stability was determined through thermogravimetric analysis (TGA). TGA is a thermal analysis technique that involves measuring a sample mass change in a controlled atmosphere as the temperature increases. The derivative curve that indicates the starting point of thermal degradation is referred to as the derivative thermogravimetric (DTG) curve.

2.6. Scanning Electron Microscopy (SEM)

The morphology of the polymer composites was evaluated using scanning electron microscopy (SEM; JEOL JCM-7000). The film sheets of the samples were coated with a thin layer of gold to enhance conductivity, and the surface morphology was examined by SEM at an accelerating voltage of 5 kV. The observations were made at various magnifications to capture detailed structural features.

3. RESULTS AND DISCUSSION

3.1. ATR-FTIR Analysis

ATR-FTIR spectroscopy investigated the chemical structures and molecular interactions of polylactic acid (PLA) and its composites. Figure 1 presents the ATR-IR spectra of PLA and its composites before and after incorporating MWCNTs and PEGs. The ATR-IR spectra of the PLA/MWCNT/PEG composites closely resemble those of neat PLA, indicating that the addition of PEGs does not significantly alter the structural characteristics. Similarly, the presence of MWCNTs has a minimal impact on the characteristic peaks of PLA. The similarity in the ATR-IR spectra across the samples suggested that their molecular structures remained unchanged.

The PLA spectrum revealed four primary regions: symmetric and asymmetric –CH stretching of CH_3 at 2995–2804 cm^{-1}, –C=O stretching at 1750–1745 cm^{-1}, symmetric and asymmetric aliphatic C–H bending at 1456–1353 cm^{-1}, and –C–O– stretching at 1145–1093 cm^{-1} [12, 23, 24].

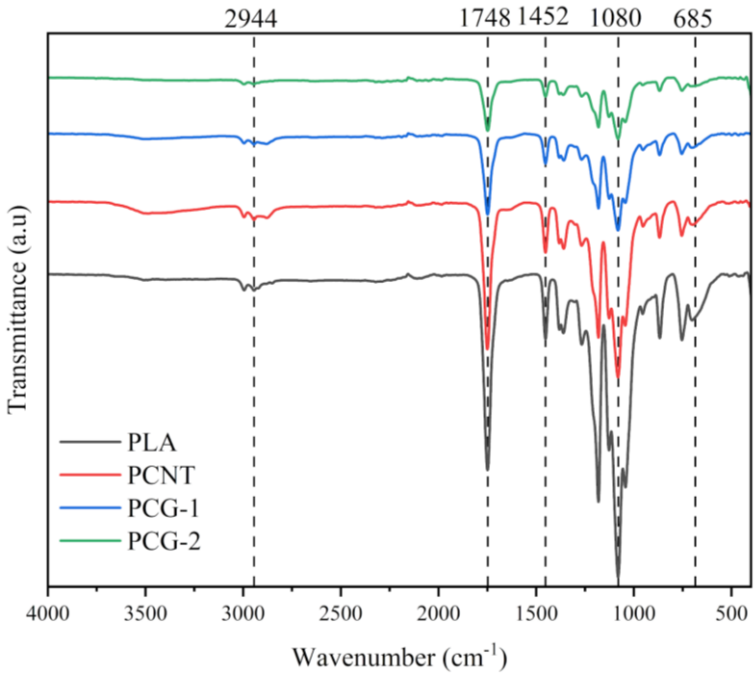

Figure 1. ATR-IR spectra of PLA and its composites.

Additionally, the peaks at 752 cm^{-1} and 873 cm^{-1} correspond to –C–C– stretching in the crystalline and amorphous phases of PLA, respectively [21, 25]. Even after incorporating MWCNTs and PEG, the characteristic peaks of PLA remain dominant, with no new peaks appearing. This consistency is expected, as MWCNTs do not possess strong functional groups that would form a robust interface with the polymer matrix. Consequently, no new functional groups were observed. Thus, any changes in the properties of the nanocomposites can be attributed to physical interactions between the MWCNTs and the PLA/PEG matrix, as well as charge transfer interactions between the conjugated surfaces of the MWCNTs and the PLA/PEG particles. However, a notable peak shift occurs at 1748 cm^{-1}, attributed to the interaction between the C=O groups in PLA and the –OH groups in PEG through strong hydrogen bonds [7, 12], as shown in Figure 2. This shift indicates that the presence of PEG significantly influences the molecular interactions within the composite.

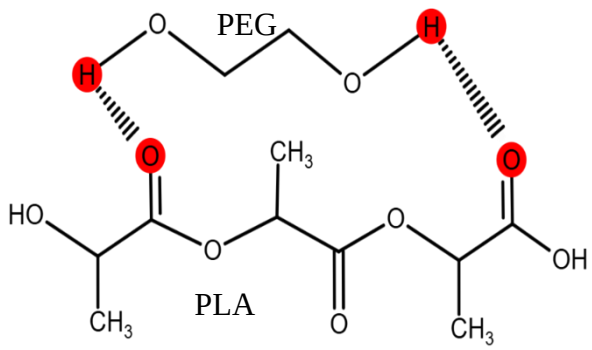

Figure 2. Possible interaction between PLA and the PEG polymer.

3.2.DSC Analysis

DSC measurements were performed to investigate the thermal properties and melting/crystallization behavior of the composites by mixing PLA, MWCNTs, and PEG polymers. The first DSC heating curve of PLA and its composites obtained with the masterbatch blending method is shown in Figure 3 (a). In the DSC curve for all the samples, three transition points can be observed, namely, the glass transition (T_g), cold crystallization (T_{cc}), and melting (T_m) temperatures, which are presented sequentially. Figure 3 (b) shows the degree of crystallinity (X_c). The DSC curves in Figure 3 (a) illustrate the thermal properties of the samples, which are utilized to calculate various shape memory polymer parameters. For neat PLA, the T_g is 57 °C, the T_{cc} is 104 °C, the T_m is 158.5 °C, and the ΔH_m (melting enthalpy) is 16.1 J/g. In contrast, the DSC curve of the PCNT composite displays three distinct peaks at 59 °C, 107.2 °C, and 159.5 °C, with an increase in the ΔH_m value of 18.3 J/g. The addition of nanofillers (MWCNTs) restricts the free volume of the polymer matrix, leading to enhancements in the T_g, T_m, and ΔH_m.

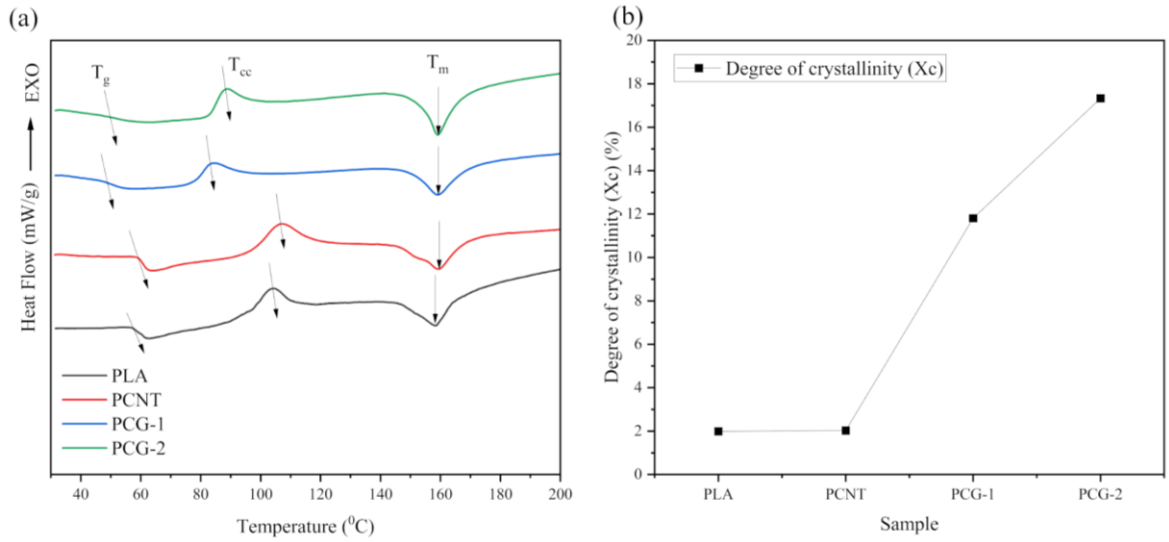

Figure 3. (a) DSC curves and (b) degree of crystallinity of the PLA composites.

The PEGs employed in this study exhibit T_m values ranging from 39 to 63 °C [26]. Since the signal at approximately 57 °C encompasses both the T_m of PEG and the T_g of PLA, it appears as a broad peak in the DSC curve. The T_g values for the PCG-1 and PCG-2 samples decreased, which can be attributed to the increased chain mobility induced by the plasticizing effects of PEG [27]. Additionally, the reduction in T_{cc} suggested that PEG facilitates the easier rearrangement of PLA chains into a crystalline structure, indicating good compatibility between PLA and PEG [28]. Furthermore, while the T_m values of the PCG-1 and PCG-2 samples remained relatively constant with the addition of PEGs, a result consistent with findings from other research [10], and the ΔH_m values increased to 19.8 J/g and 24.6 J/g, respectively. This increase is likely due to the combined presence of PEG and the loading of MWCNTs, which promote crystallization and enhance the thermal properties of the composites.

The degrees of crystallinity for the polymer composites were calculated using DSC data and are illustrated in Figure 3(b). Pure PLA exhibited very low crystallinity, measured at 1.9%. After adding 1% MWCNTs, the crystallinity slightly increased to 2%. Notably, the composite containing 14% PEG with a Mw of 10,000 achieved the highest crystallinity among the samples, reaching 17.3%. This finding suggests that incorporating PEG with a higher Mw within the composite significantly enhances the degree of crystallinity. Specifically, the 14% PEG 10,000 composite demonstrated peak crystallinity, indicating that PEG at this concentration and molecular weight notably improved the crystalline structure of the composite. These findings suggest that such composites could be highly suitable for packaging applications [12], where thermal resistance is crucial. Moreover, when compared to other biopolymer blends, such as PLA/ESO/MWCNT (20% ESO and 3% MWCNT-

COOH), which achieved a crystallinity of 18% [29], the PLA/MWCNT/PEG composite demonstrated good thermal properties and comparable crystallinity improvements with a lower filler content. These results highlight the potential of PLA/MWCNT/PEG composites in packaging applications and pave the way for further research into optimizing blend ratios and processing conditions to maximize performance.

The synergistic effect of the hybrid MWCNT/PEG significantly enhances the crystallization rate of the PLA phase during the masterbatch blending process. The greater ΔH_m and X_c observed in the PLA/MWCNT/PEG composites compared to those in pure PLA can be attributed to the increased number of nucleation sites and accelerated crystallization rate facilitated by the presence of MWCNTs and PEG [3, 6]. In general, plasticizers interact with polymer chains at the molecular level, as demonstrated by FTIR analysis (Figure 2). This interaction enhances the viscoelastic response of the polymer. The incorporation of plasticizers increases the mobility of polymer chains, thereby accelerating the crystallization rate by lowering the energy required for the chain folding process during crystallization [28].

3.3.Thermogravimetric Analysis

To assess the impact of reinforcement materials on the thermal stability of polymer matrices, it is essential to thoroughly investigate the thermal stability of polymer composites. The thermal stability and degradation characteristics of the neat PLA, PLA/MWCNT, and PLA/MWCNT/PEG composites were analyzed using thermogravimetric analysis (TGA) and derivative thermogravimetry (DTG). The relevant data for neat PLA and its composites are presented in Table I. Figures 4(a) and 4(b) illustrate the TGA and DTG results, respectively, over the temperature range of 30 °C to 550 °C. To study the thermal stability behavior of these materials, the temperature at 5 wt% weight loss ($T_{5\%}$), the temperature at 50 wt% weight loss ($T_{50\%}$), the maximum decomposition temperature (T_{max}), and the residue remaining after the maximum temperature study are listed.

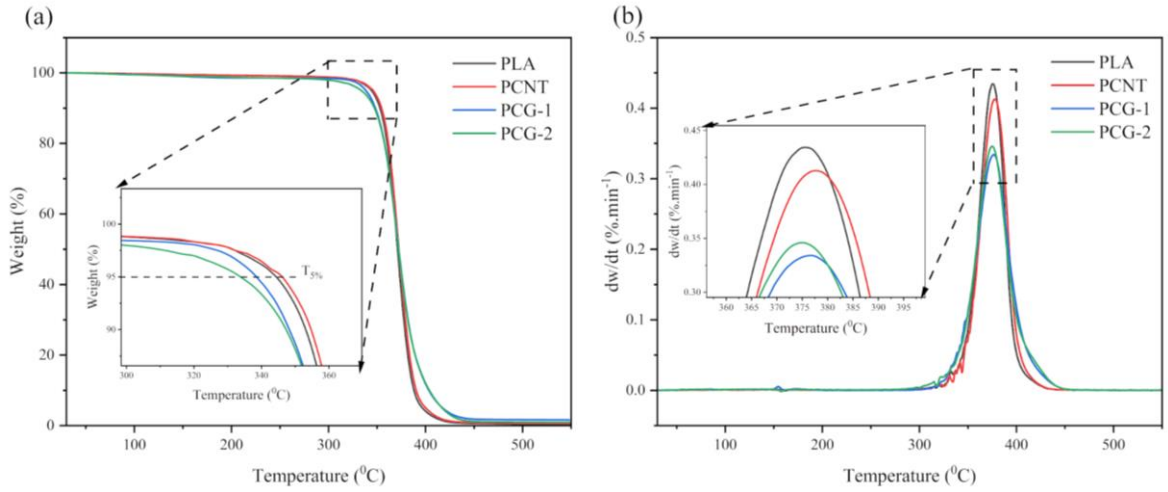

Figure 4. (a) TGA and (b) DTG curves of PLA and its composites.

Observations indicated that PLA and its composites displayed similar thermogravimetric profiles, characterized by a one-step threshold weight loss. The significant weight loss for PLA and its composites occurred between 300 °C and 400 °C, primarily due to the degradation of PLA. Neat PLA exhibited a single-step weight loss with a $T_{5\%}$ at approximately 344.35 °C. According to the DTG analysis, the T_{max} of PLA was observed at 375 °C. The incorporation of MWCNTs into the PLA matrix enhanced the thermal stability of the material, as evidenced by an increase in $T_{5\%}$. Conversely, the presence of PEGs in the PLA/MWCNT/PEG composites resulted in a decrease in thermal stability, with the degradation curves shifting to lower temperatures, indicating accelerated degradation.

TABLE I. Thermogravimetric analysis of PLA and its composites.

Sample	$T_{5\%}$(ºC)	$T_{50\%}$(ºC)	T_{max} (ºC)	Residue (%)
PLA	344.35	371.20	375.00	0.40
PCNT	346.15	372.50	378.80	0.65
PCG-1	338.49	372.42	376.55	1.62
PCG-2	333.74	372.20	375.00	0.95

At 50% weight loss ($T_{50\%}$), the trend remained consistent, and the inclusion of PEG had a plasticizing effect on the composites, reducing their rigidity. The stable $T_{50\%}$ evidences this compared to the unfilled PEG composites. The $T_{50\%}$ of PCNT and the composites with PEG (PCG-1 and PCG-2) differed by only 0.3 °C, indicating that the thermal stability of both composites was maintained despite the presence of the plasticizer. The T_{max} slightly decreased when 14 wt% PEG was incorporated into the composites. However, the amount of residue remaining after reaching the maximum temperature increased in the PCG phase. This effect is associated with the increased crystallinity of the polyester due to the presence of PEGs, as confirmed by DSC experiments. The amount of residue decreased with increasing PEG molecular weight (Mw), with the highest residue observed in the composite containing PEG with a molecular weight of 1,000.

3.4.Morphology Observation

Figure 5 shows SEM micrographs of the surfaces of the PLA and PCNT samples at 1,000× and 3,000× magnification. The PLA sample, shown in Figure 5(a), exhibits a smooth fracture surface with minimal plastic deformation, characteristic of its brittle and stiff nature. In contrast, the addition of MWCNTs significantly increased the surface roughness of the composite, as illustrated in Figure 5(b). This image reveals a network of fine nanotubes arranged randomly, densely, and interconnectedly. Notably, the MWCNTs are uniformly distributed and well dispersed within the PLA matrix, with no signs of aggregation. This uniform dispersion can be attributed to using an ultrasonic homogenizer while preparing the PCNT solution. The combination of solvent-cast PLA/MWCNTs in chloroform and ultrasonic stirring generates high shear stress within the PLA solution, facilitating an even and uniform dispersion of MWCNTs in the polymer matrix. Furthermore, it aligns with other research findings that high-power dispersion techniques, such as ultrasonic and high-speed shearing methods, are effective and convenient for enhancing the distribution of nanosized fillers in polymer matrices [30].

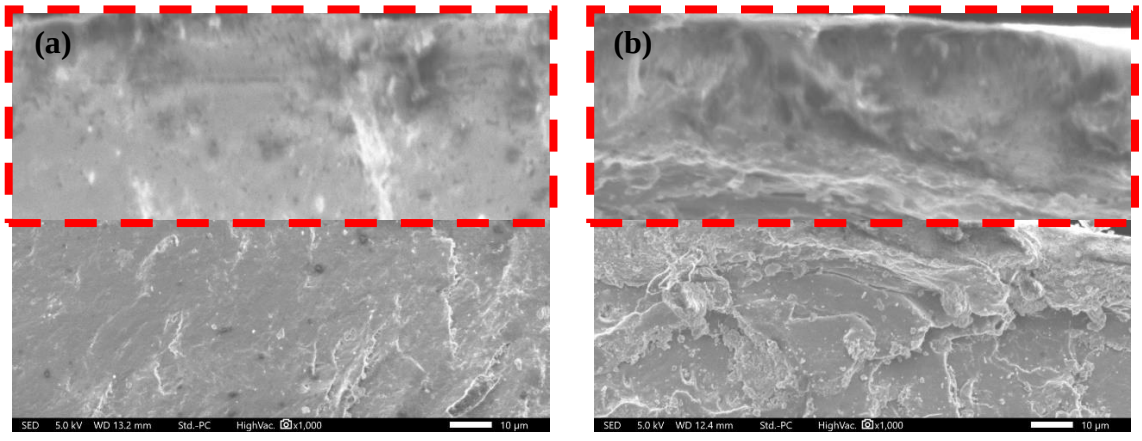

Figure 5. SEM cross-sections at 1000× magnification (in the red box, 3000×) for (a) PLA and (b) PCNT.

4. CONCLUSIONS

The masterbatch blending method was employed to examine the impact of PEGs on the

properties of the PLA/MWCNT/PEG polymer composites. The ATR-FTIR analysis revealed significant changes in the carbonyl group peak at 1748 cm^{-1}. The intensity of these spectral peaks increased with the molecular weight (Mw) of PEG, suggesting substantial chemical interactions between PLA and PEG at higher PEG molecular weights. Independent of the PEG Mw, the glass transition temperature (T_g) of the composites decreased. At the same time, the crystallinity increased, leading to enhanced ductility compared to that of the PLA/MWCNT (PCNT) composites. These effects are attributed to strong chemical interactions between PLA, MWCNTs, and PEG and the formation of a homogeneous matrix following the masterbatch blending process. According to DSC analysis, the PCG-2 composite exhibited the highest crystallinity, which correlates with the enhanced ductility observed. The addition of PEG as a plasticizer contributed to this increase in crystallinity, as evidenced by the maximum ΔH_m recorded for the PCG-2 composite at 24.6 J/g. The TGA study demonstrated the excellent thermal stability of the composites, with weight loss occurring at higher temperatures, indicating delayed degradation. The PLA/MWCNT/PEG (PCG) composites maintained good thermal stability among the analyzed composites. Specifically, the degradation temperatures remained consistent even with adding PEG with molecular weights of 1,000 and 10,000 g/mol. The combination of solvent-cast PLA/MWCNTs in chloroform and ultrasonic stirring generates substantial shear stress within the PLA solution, facilitating the uniform dispersion of the MWCNTs throughout the PLA matrix.

Acknowledgments

We would like to express our sincere gratitude to Universitas Sebelas Maret for their support, including the provision of laboratory facilities and research funding.

References

[1] D. Marlina, H. Sato, H. Hoshina, and Y. Ozaki, "Intermolecular interactions of poly(3-hydroxybutyrate-co-3-hydroxyvalerate) (P(HB-co-HV)) with PHB-type crystal structure and PHV-type crystal structure studied by low-frequency Raman and terahertz spectroscopy," *Polymer (Guildf).*, vol. 135, pp. 331–337, Jan. 2018, doi: 10.1016/j.polymer.2017.12.030.

[2] N. Karimpour-Motlagh *et al.*, "An experimental and theoretical mechanistic analysis of thermal degradation of polypropylene/polylactic acid/clay nanocomposites," *Polym. Adv. Technol.*, vol. 30, no. 11, pp. 2695–2706, Nov. 2019, doi: 10.1002/pat.4699.

[3] S. Jia, D. Yu, Y. Zhu, Z. Wang, L. Chen, and L. Fu, "Morphology, Crystallization and Thermal Behaviors of PLA-Based Composites: Wonderful Effects of Hybrid GO/PEG via Dynamic Impregnating," *Polymers (Basel).*, vol. 9, no. 10, p. 528, Oct. 2017, doi: 10.3390/polym9100528.

[4] S. Djellali, T. Sadoun, N. Haddaoui, and A. Bergeret, "Viscosity and viscoelasticity measurements of low density polyethylene/poly(lactic acid) blends," *Polym. Bull.*, vol. 72, no. 5, pp. 1177–1195, May 2015, doi: 10.1007/s00289-015-1331-6.

[5] A. Bouzouita *et al.*, "Design of highly tough poly(l-lactide)-based ternary blends for automotive applications," *J. Appl. Polym. Sci.*, vol. 133, no. 19, May 2016, doi: 10.1002/app.43402.

[6] H. Norazlina and Y. Kamal, "Elucidating the plasticizing effect on mechanical and thermal properties of poly(lactic acid)/carbon nanotubes nanocomposites," *Polym. Bull.*, vol. 78, no. 12, pp. 6911–6933, 2021, doi: 10.1007/s00289-020-03471-2.

[7] N. Sundar, S. J. Stanley, S. A. Kumar, P. Keerthana, and G. A. Kumar, "Development of dual purpose, industrially important PLA–PEG based coated abrasives and packaging materials," *J. Appl. Polym. Sci.*, vol. 138, no. 21, pp. 1–18, 2021, doi: 10.1002/app.50495.

[8] M. Chalid, G. Gustiraharjo, A. I. Pangesty, A. Adyandra, Y. Whulanza, and S. Supriadi, "Effect of PEG Incorporation on Physicochemical and in vitro Degradation of PLLA/PDLLA Blends: Application in Biodegradable Implants," *J. Renew. Mater.*, vol. 11, no. 7, pp. 3043–3056, 2023, doi: 10.32604/jrm.2023.026788.

[9] A. F. Ahmad *et al.*, "Biodegradable poly (lactic acid)/poly (ethylene glycol) reinforced multi-walled carbon nanotube nanocomposite fabrication, characterization, properties, and applications," *Polymers (Basel).*, vol. 12, no. 2, pp. 0–22, 2020, doi: 10.3390/polym12020427.

[10] S.-F. Wang, Y.-C. Wu, Y.-C. Cheng, and W.-W. Hu, "The Development of Polylactic Acid/Multi-Wall

Carbon Nanotubes/Polyethylene Glycol Scaffolds for Bone Tissue Regeneration Application," *Polymers (Basel).*, vol. 13, no. 11, p. 1740, May 2021, doi: 10.3390/polym13111740.

[11] S. Wang, R. Wu, J. Zhang, Y. Leng, and Q. Li, "PLA/PEG/MWCNT composites with improved processability and mechanical properties," *Polym. Technol. Mater.*, vol. 60, no. 4, pp. 430–439, 2021, doi: 10.1080/25740881.2020.1811324.

[12] H. Shin, S. Thanakkasaranee, K. Sadeghi, and J. Seo, "Preparation and Characterization of Ductile PLA/PEG Blend Films for Eco-Friendly Flexible Packaging Application," *SSRN Electron. J.*, vol. 34, no. September, pp. 1–10, 2022, doi: 10.2139/ssrn.4164380.

[13] J. M. Raquez, Y. Habibi, M. Murariu, and P. Dubois, "Polylactide (PLA)-based nanocomposites," *Prog. Polym. Sci.*, vol. 38, no. 10–11, pp. 1504–1542, 2013, doi: 10.1016/j.progpolymsci.2013.05.014.

[14] X. Feng, X. Wang, W. Cai, S. Qiu, Y. Hu, and K. M. Liew, "Studies on Synthesis of Electrochemically Exfoliated Functionalized Graphene and Polylactic Acid/Ferric Phytate Functionalized Graphene Nanocomposites as New Fire Hazard Suppression Materials," *ACS Appl. Mater. Interfaces*, vol. 8, no. 38, pp. 25552–25562, 2016, doi: 10.1021/acsami.6b08373.

[15] N. Karimpour-Motlagh *et al.*, "Influence of polypropylene and nanoclay on thermal and thermo-oxidative degradation of poly(lactide acid): TG-FTIR, TG-DSC studies and kinetic analysis," *Thermochim. Acta*, vol. 691, no. July, p. 178709, 2020, doi: 10.1016/j.tca.2020.178709.

[16] P. Colomban, "Understanding the nano- and macromechanical behaviour, the failure and fatigue mechanisms of advanced and natural polymer fibres by Raman/IR microspectrometry," *Adv. Nat. Sci. Nanosci. Nanotechnol.*, vol. 4, no. 1, p. 013001, Dec. 2013, doi: 10.1088/2043-6262/4/1/013001.

[17] S.-F. Yao, X.-T. Chen, and H.-M. Ye, "Investigation of Structure and Crystallization Behavior of Poly(butylene succinate) by Fourier Transform Infrared Spectroscopy," *J. Phys. Chem. B*, vol. 121, no. 40, pp. 9476–9485, Oct. 2017, doi: 10.1021/acs.jpcb.7b07954.

[18] R. Caban, "FTIR-ATR spectroscopic, thermal and microstructural studies on polypropylene-glass fiber composites," *J. Mol. Struct.*, vol. 1264, p. 133181, 2022, doi: 10.1016/j.molstruc.2022.133181.

[19] C. Qian, Y. Zhao, Z. Wang, L. Liu, and D. Wang, "Probing the difference of crystalline modifications and structural disorder of isotactic polypropylene via high-resolution FTIR spectroscopy," *Polymer (Guildf).*, vol. 224, p. 123722, May 2021, doi: 10.1016/j.polymer.2021.123722.

[20] Y. Qin *et al.*, "Interfacial interaction enhancement by shear-induced β-cylindrite in isotactic polypropylene/glass fiber composites," *Polymer (Guildf).*, vol. 100, pp. 111–118, Sep. 2016, doi: 10.1016/j.polymer.2016.08.016.

[21] M. Vosough Kia, M. Ehsani, S. E. Hosseini, and G. H. Asadi, "Fabrication and characterization of transparent nanocomposite films based on poly (lactic acid)/polyethylene glycol reinforced with nano glass flake," *Int. J. Biol. Macromol.*, vol. 254, no. P1, p. 127473, 2024, doi: 10.1016/j.ijbiomac.2023.127473.

[22] B. Xue, Z. Cheng, S. Yang, X. Sun, L. Xie, and Q. Zheng, "Extensional flow-induced conductive nanohybrid shish in poly(lactic acid) nanocomposites toward pioneering combination of high electrical conductivity, strength, and ductility," *Compos. Part B Eng.*, vol. 207, no. September 2020, p. 108556, 2021, doi: 10.1016/j.compositesb.2020.108556.

[23] B. W. Chieng, N. A. Ibrahim, W. M. Z. W. Yunus, M. Z. Hussein, Y. Y. Then, and Y. Y. Loo, "Effects of graphene nanoplatelets and reduced graphene oxide on poly(lactic acid) and plasticized poly(lactic acid): A comparative study," *Polymers (Basel).*, vol. 6, no. 8, pp. 2232–2246, 2014, doi: 10.3390/polym6082232.

[24] X. Huang, X. Ge, L. Zhou, and Y. Wang, "Eugenol embedded zein and poly(lactic acid) film as active food packaging: Formation, characterization, and antimicrobial effects," *Food Chem.*, vol. 384, no. November 2021, p. 132482, 2022, doi: 10.1016/j.foodchem.2022.132482.

[25] L. Wang, Y. Zhang, Q. Xing, J. Xu, and L. Li, "Quality and microbial diversity of homemade bread packaged in cinnamaldehyde loaded poly(lactic acid)/konjac glucomannan/wheat gluten bilayer film during storage," *Food Chem.*, vol. 402, no. April 2022, 2023, doi: 10.1016/j.foodchem.2022.134259.

[26] P. Johansson *et al.*, "Cycling stability of poly(ethylene glycol) of six molecular weights: Influence of thermal conditions for energy applications," *ACS Appl. Energy Mater.*, vol. 3, no. 11, pp. 10578–10589, 2020, doi: 10.1021/acsaem.0c01621.

[27] M. Bijarimi, S. Ahmad, R. Rasid, M. A. Khushairi, and M. Zakir, "Poly(lactic acid) / Poly(ethylene glycol) blends: Mechanical, thermal and morphological properties," in *AIP Conference Proceedings*, 2016, p. 020002. doi: 10.1063/1.4945957.

[28] I. G. Athanasoulia and P. A. Tarantili, "Preparation and characterization of polyethylene glycol/poly(L-lactic acid) blends," in *Pure and Applied Chemistry*, Crete: De Gruyter, 2017, pp. 141–152. doi: 10.1515/pac-2016-0919.

[29] S. Raghunath, S. Kumar, S. K. Samal, S. Mohanty, and S. K. Nayak, "PLA/ESO/MWCNT nanocomposite: a study on mechanical, thermal and electroactive shape memory properties," *J. Polym. Res.*, vol. 25, no. 5, p. 126, 2018, doi: 10.1007/s10965-018-1523-5.

[30] S. G. Park, A. Abdal-Hay, and J. K. Lim, "Biodegradable poly(lactic acid)/multiwalled carbon nanotube nanocomposite fabrication using casting and hot press techniques," *Arch. Metall. Mater.*, vol. 60, no. 2, pp. 1557–1559, 2015, doi: 10.1515/amm-2015-0172.